Hindawi
Advances in Civil Engineering
Volume 2024, Article ID 4505901, 20 pages
https://doi.org/10.1155/2024/4505901

Research Article

Enhancing Seismic Performance: A Comprehensive Study on Masonry and Reinforced Concrete Structures Considering Soil Properties and Environmental Impact Assessment

Benjamin Labar, Nurullah Bektaş, and Orsolya Kegyes-Brassai

Department of Structural Engineering and Geotechnics, Széchenyi István University, 9026, Győr, Hungary

Correspondence should be addressed to Benjamin Labar; labar.benjamin.beeior@hallgato.sze.hu

Received 2 January 2024; Revised 7 April 2024; Accepted 12 April 2024; Published 30 April 2024

Academic Editor: Edén Bojórquez

Approximately 20,000 people are killed annually on average by building and infrastructure collapses and failures caused by seismic activities. In earlier times, seismic design codes and specifications set minimal requirements for life safety performance levels. Earthquakes can be thought of as recurring events in seismically active areas, with severity states ranging from serviceability to ultimate levels. Buildings designed in accordance with site-specific response spectra, which take into account soil properties based on ground motion amplification data, are better at withstanding such forces and serving their design purposes. This study aims to investigate the site response of reinforced and masonry buildings, considering the effect of soil properties based on the amplification of ground motion data, and to compare the life cycle assessment of the buildings under consideration based on the design and the site-specific response spectrum. In terms of soil properties and site-specific response spectra, STRATA is used to determine the site-specific response for the considered locations for a return period of 475 years for 100 realizations based on the randomization of site properties. For structural analysis, AxisVM software, which is a compatible finite element analysis, is used for building design and analysis, generating comparative results based on the design- and site-specific spectra. To determine and identify potential failures in the model, response spectra were applied to understand the difference in horizontal deflection in two different instances (for elastic design- and site-specific spectra). After building design and analysis is performed, a life cycle analysis in terms of environmental impact assesments using OpenLCA and IdematLightLCA is done. This is done to ascertain the additional expenses in terms of ecocosts and carbon footprints on some failed elements in the structure which are required to make the buildings more resilient when the site-specific response spectrum is applied and to compare the potential economic losses that may occur based on ecological costs. The study presents a comprehensive investigation into the seismic response of masonry and reinforced concrete buildings in Győr, Hungary, incorporating advanced geophysical techniques like multichannel surface wave (MASW) and structural analysis software, AxisVM. Additionally, tailored retrofitting strategies are explored to enhance structural resilience in seismic-prone regions. Significant ground amplifications in soil properties across different profiles are revealed, emphasizing the effectiveness of these strategies in reducing structural deflection and improving resilience. Highlights of the results are observed where the site-specific response spectra are higher than the EC8 design response spectrum. Furthermore, the research underscores the substantial environmental impact, considering both ecocosts and CO_2 emissions associated with retrofitting measures, highlighting the importance of sustainable structural interventions in mitigating seismic risks.

1. Introduction

The annual average death toll from earthquakes associated with building and infrastructure collapses and failures cumulatively is approximately 20,000 people. Historically, seismic building codes and design specifications have established minimum requirements for life safety and the prevention of collapse. In areas prone to seismic activity, earthquakes are reoccurring events with severity states between serviceability and ultimate levels. The local site response spectra are greatly affected by the thickness, density, and other physical properties of the soil, which are significant in the evaluation of seismic response [1–3]. Since the subsurface of seismic propagation and amplification of the soil significantly affect the seismic response of

structures, the effects of soil conditions and properties should be considered in the evaluation of the seismic response of buildings [1, 2, 4, 5]. Numerous researchers [4, 6–9] studied that the amplification of site response from the bedrock to the surface is greatly influenced by the type of soil, indicating that the risk in hard rocky soils is lower compared to soft soils, as seismic amplification at the surface is generally greater than the amplification at bedrock in most instances. These seismic amplification forces that propagate from the bedrock to the surface contribute to the damage and destruction of buildings, leading to environmental consequences and significant impacts [5, 10]. The primary goal of earthquake risk analysis studies is to forecast the parameters needed for the design of earthquake-resistant structures. One of the most important parameters among these is the lateral peak ground acceleration (PGA), which affects structures during earthquakes. PGA is influenced by dynamic soil amplifications, which show the ratio of earthquake acceleration to the surface of the ground surface from bedrock to the surface [5, 11].

According to Pettinga and Priestley [12], the seismic design process primarily relies on force-based dynamic amplification due to soil properties. This involves applying external forces (horizontal push and pull forces, shear forces, etc.) to the structure, equivalent to the inertial forces caused by ground accelerations. This design approach mainly focuses on the first mode response of the structure, assuming that most of the structural behavior can be captured by this mode. However, if certain limitations in structural behavior are not met, requirements for multimodal analysis are imposed. This means that additional modes of vibration are considered to ensure a more comprehensive evaluation of the structure's response to seismic forces. Also, in a separate research, Bijukchhen et al. [13] and D'Amico et al. [14] noted that it is important to recognize that seismic waves can undergo amplification when traveling through certain types of soil or unconsolidated sediments. Consequently, an earthquake that may appear relatively harmless when experienced on solid ground can pose a significant threat in areas with soft or unstable soils. This amplification phenomenon can lead to higher levels of ground shaking and amplifications, which in turn can result in severe damage to infrastructure.

The assessment of natural hazard impacts and seismic excitations on the structural integrity of buildings has become a popular approach nowadays for investigating resilience and the relationship between structures and soil [15]. Investigations into the effect of soil–structure interactions (SSIs) can offer valuable technical support for improving conventional seismic design practices and methods for evaluating urban earthquake damage [16]. To this end, the evaluation of building structures traditionally assumes that the building's foundation is rigid, disregarding the influence of local soil conditions on its response [17]. However, the destructive impact of earthquakes has drawn attention to the seismicity of the SSI in residentail and multistory buildings [17]. Interestingly, in earthquake damage evaluations in cities or specific regions, the effect of SSI on structural responses has often been overlooked to improve computational efficiency [18]. Nevertheless, recent studies by scholars such as [17–19] have emphasized the significance of considering SSI. They have observed that the horizontal movement and rotation of the foundations can amplify the lateral deformation and story drift of superstructures, leading to adverse conditions for structural seismic vulnerability.

In the assessment of building vulnerability to seismic events in Nepal, as noted by Karki et al. [5], many damages were attributed to the neglect of underlying soil properties. Postanalysis revealed some degree of variation in the fundamental building period when considering soil properties. The ground motions derived from this consideration show that the design levels specified in the Nepalese building codes have been exceeded [20]. Also, in a joint postearthquake field reconnaissance of the 2023 Turkey–Syria earthquake conducted by the Earthquake Engineering Research Institute (EERI), the Geotechnical Extreme Events Reconnaissance (GEER), and the European Centre for Training and Research in Earthquake Engineering (EUCENTRE), site response analysis was conducted in the affected areas using one-dimensional equivalent linear analysis, and the results indicated that the site-specific response and the PGA analysis demonstrated spectral acceleration of up to 0.85 g, which was 1.8 times greater than the recommended national design spectrum specified by the 2007 Turkey seismic design code [21]. In a similar study, Aldemir et al. [22] analyzed a hybrid building to assess the seismic performance of unreinforced masonry buildings. This approach integrates finite element and equivalent frame methods to analyze the global behavior, taking into consideration geometrical shapes. However, the analysis did not incorporate soil properties. In additional research, Araz [23, 24] emphasized various techniques for vibration control in buildings to attain lower maintenance costs during both passive and active seismic forces. This involved the introduction of tuned mass dampers (TMDs) as control devices between the structure and various soil types, including dense soil, medium soil, and soft soil. Subsequent findings demonstrated significant control over the peak horizontal displacement, resulting in no displacement in the optimized 40-story model. However, it was observed that the optimum frequency ratio decreases with a reduction in soil stiffness. Garini et al. [25] carried out a detailed seismic classifer toolbox (SCT) investigation of strategic positions near public buildings in the heart of Mexico City by considering four different sites and six points on each site. The resulting amplification revealed that the spectral accelerations were approximately 0.8–1.0 g, much higher than the spectral values of 0.20 g. Larger dominant periods of greater than 2 s for each amplification function were also recorded, confirming the occurrence of resonance at the fundamental natural period of each particular soil stratum, which was noticed to have been far different between the amplification functions of the east–west and north–south components. Amendola and Pitilakis [26], on the issue of soil amplifications, highlighted that large seismic risk assessment applications still suffer from various setbacks related to soil responses, indicating that most assessments in many countries, such as Italy, still neglect important hazard factors such as site amplification (SAmp) by generalizing the same type A soil to correspond to the stiff soil category for the entire country. The impact of an earthquake on infrastructure is influenced by

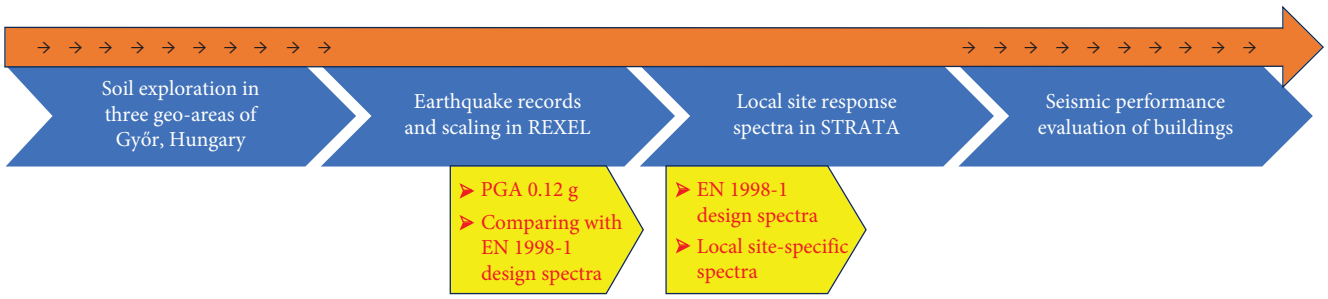

Figure 1: Flowchart of seismic vulnerability assessment.

various factors, including source characteristics, path conditions, and site conditions. Although the magnitude of the earthquake is a key parameter, the significance of site conditions should not be overlooked. In fact, the nature of the ground on which a structure is built can greatly influence the extent of the damage caused by an earthquake [13, 14].

The seismic forces generated from the bedrock to the surface can lead to collapse and structural issues, including cracks and soil liquefaction. Building systems may experience reduced structural capacity and durability due to seismic forces, environmental factors like climate change, landforms, and human-induced activities [27–29]. Addressing such defects and performance losses involves considering options like demolition or strengthening [27–30]. However, opting for building strengthening requires ensuring structural sustainability of these buildings, which is an unavoidable task. This involves assessing the ecological cost and carbon footprint to make environmentally responsible choices in the selection of the appropriate materials [27]. In the building sector, there is growing attention towards reducing the environmental impact of products through life cycle analysis, which evaluates their effects from manufacturing to disposal or recycling. Reusing products and selecting, deconstructing, and reconstructing building components for retrofitting and redesigning purposes are gaining prominence as strategies for reducing environmental impact effects [31, 32]. In addition to economic considerations, the process of demolishing and rebuilding structures affected by seismic and other structural actions raises substantial environmental issues [4, 10, 21]. As highlighted by Clemett [27], approximately 40% of the European countries' total energy consumption and greenhouse gas (GHG) emissions stem from the building sector. Within this percentage, a portion of the emissions can be traced to the demolition and reconstruction of buildings.

Building upon these challenges and considerations, this study offers an approach by integrating geophysical techniques, such as multichannel surface wave (MASW), with advanced structural analysis to comprehensively evaluate the seismic response of buildings in Győr, Hungary. Additionally, the investigation into tailored retrofitting strategies highlights the innovative methods employed to enhance structural resilience in seismic-prone regions. The study reveals significant variations in ground motion amplification across different soil profiles and underscores the effectiveness of tailored retrofitting strategies in reducing structural deflection and enhancing overall resilience to seismic hazards. Furthermore, the research highlights the substantial environmental impact considering both ecocosts and CO_2 emissions associated with retrofitting measures, emphasizing the importance of sustainable structural interventions in mitigating seismic risks.

2. Presentation of Methodology

The study focuses on comprehensively investigating the performance of two buildings (unreinforced masonry and reinforced concrete buildings), with similar properties such as layout, height, and number of stories considering soil properties based on ground motion data amplification and how these buildings behave under various loading conditions, while also taking into account factors such as their environmental impact and the potential for materials and methods for retrofitting failed elements of the buildings, and their interaction with the supporting soil. This analysis has been conducted using wave propagation analysis across the soil layers (site-specific spectrum from the soil conditions), which will allow the propagation of ground motion data. Additionally, the study will examine the linear horizontal deformations and mode shapes in line with the propagation of the soil properties by utilizing finite element software as illustrated in Figure 1.

To enable the use of actual earthquake records as input for nonlinear dynamic analysis, the REXEL software tool is used to generate and scale nonlinear dynamic earthquake records following the specification of Eurocode 8 [33]. This process aids in the proper selection of seismic input and earthquake records by utilizing fundamental probabilistic seismic hazard parameters, considering factors such as soil types, location, peak ground acceleration, and distance. REXEL identifies suitable sets of earthquake records suitable for various structural applications [33]. To accomplish these objectives, soil profiles obtained from three different sites (OBI mellet, Kekszgyár, and Víztükör ltp) using the MASW method were considered in terms of the site PGA, varying thickness, unit weight, and share wave velocities, respectively. Earthquakes parameters scaled from REXEL in the time domain were employed for this purpose, facilitating the application of random vibration theory (RVT) were imported into STRATA software, a one-dimensional equivalent site response analysis software considering 100 realizations and a return period of 475 years based on the randomization of site properties, to ascertain the site-specific response spectra based on the geotechnical soil parameters and the input earthquake records

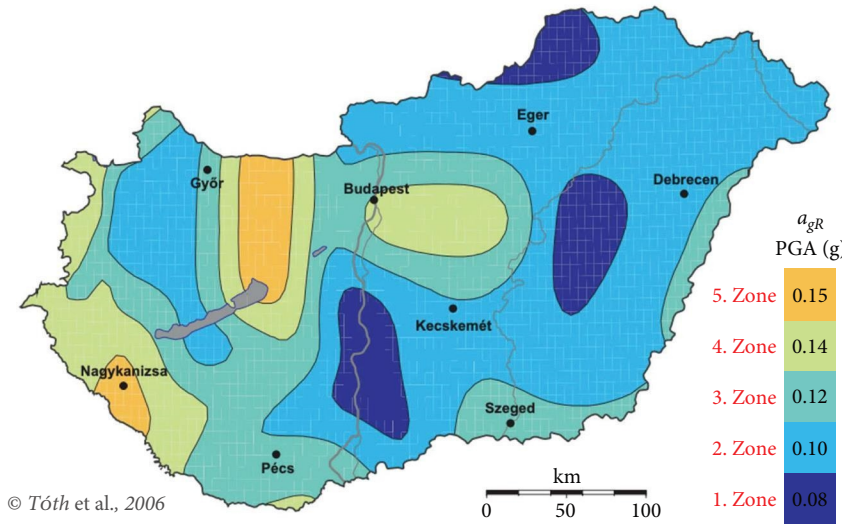

Figure 2: Seismic hazard map of Hungary [38].

obtained from REXEL [34]. Correlatively with a cutting-edge paper on ground motion selection and scaling [35], REXEL also employs a code-based selection approach and spectral matching. This approach incorporates a holistic probabilistic assessment method based on intensity measures, PGA, and distance scenarios, following EC8 requirements, while considering soil site classes A, B, and C [33, 35, 36].

Finally, AxisVM, a robust finite element software and a practical modeling tool incorporated with seismic and earthquake recording data, was deployed for structural design and analysis aiming to provide a comprehensive understanding of the behavior and performance of the buildings and their interaction with the elastic response spectrum and site-specific spectra [37].

3. Site Seismicity and Soil Properties

Since the considered masonry and reinforced concrete buildings are located in Győr, Hungary, seismicity of the site, site soil properties based on Eurocode, and corresponding design response spectrum have been provided in the following sections.

3.1. Site Seismicity. Hungary is a moderate seismicity region. The seismic activity in Hungary, as shown in the national seismic hazard map in Figure 2, indicates a 10% probability of surpassing a 50-year interval with a return period of 475 years for peak ground acceleration [38]. For the study area of Győr, situated halfway between Budapest and Vienna, an earthquake of magnitude 6.2–6.5 occurred in Komárom in 1763, which is approximately 40 km from Győr. This, by extension, has put Győr on a higher peak ground acceleration based on the microzonation of seismic hazards in Hungary. The hazard map of Hungary displays Győr's peak ground acceleration at 0.12 g, which is used in this investigation for scaling and computation of the response analysis [38, 39].

3.2. Site Soil Properties. Geotechnical engineering heavily relies on geological knowledge, as soil characteristics can exhibit significant variations even within small distances. Therefore, a thorough understanding of soil properties at a specific site is essential for geotechnical purposes. Soil originates from rock weathering and is a complex material with inherent variability [13]. Brunelli et al. [10] emphasize that due to soil complexity and variable nature, geotechnical engineers must possess deep insights into soil properties to ensure the success of engineering projects. Failures in geotechnical systems and increased construction costs can often be attributed to an inadequate understanding of geological formations and groundwater conditions. In line with the importance of soil properties, Eurocode 8 (EN 1998-1:2004 E) provides guidelines for seismic design that rely heavily on the classification of soil types. The seismic classification of soils primarily relies on the average shear wave velocity of the upper 30 m of the site, known as Vs30. Vs30 serves as an indicator of soil stiffness under moderate deformations in the upper soil layers. Eurocode 8 establishes five primary soil types and one unique one. This classification framework allows for the consideration of site-specific soil behavior in seismic design and analysis, as illustrated in Table 1.

The soil exhibits various characteristics that can be classified using commonly known terms such as gravel, sand, silt, and clays. These terms correspond to the texture of the soil, which provides insight into its visual and tactile properties. Coarse-grained soils, including sand and gravel, consist of larger particles, whereas fine-grained soils, such as clays and silts, comprise smaller particles. The distribution of particle sizes in coarse-grained soils serves as an indicator of their coarseness. Conversely, the mechanical behavior of fine-grained soils is influenced by the dominant mineral types present. Figure 3 shows that the dominant soil type for Győr is type C according to the Eurocode (EN 1998-1:2004 E) [36].

Finally, the design response spectrum considered in this study is shown in Figure 4, in which key parameters were considered based on the geological site conditions for the horizontal components of the seismic action, and the following parameters were noted based on the usage and function of the building: ag of 1.2 m/s^2 for the design ground

Table 1: Soil profile type classification for seismic amplification based on Eurocode 8 (EN 1998-1:2004 E) [36].

Ground type	General description	Average shear wave velocity to 30 m (m/s)
A	Rock or other rock-like geological formations, including at most 5 m of weaker material at the surface	>800
B	Deposits of very dense sand, gravel, or very stiff clay, at least several tens of meters in thickness, are characterized by a gradual increase in mechanical properties with depth	360–800
C	Deep deposits of dense or medium-dense sand, gravel, or stiff clay with thickness from several tens to many hundreds of meters	180–360
D	Deposits of loose-to-medium cohesionless soil (with or without some soft cohesive layers), or of predominantly soft-to-firm cohesive soil	<180
E	A soil profile consisting of a surface alluvium layer with vs values of type C or D and thickness varying between about 5 and 20 m, underlain by stiffer material with vs. > 800 m/s	—
	Deposits consisting, of or containing a layer at least 10 m thick, of soft clays/silts with a high plasticity index (PI > 40) and high-water content	<100 (indicative)
	Deposits of liquefiable soils, sensitive clays, or any other soil profile not included in types A–E	—

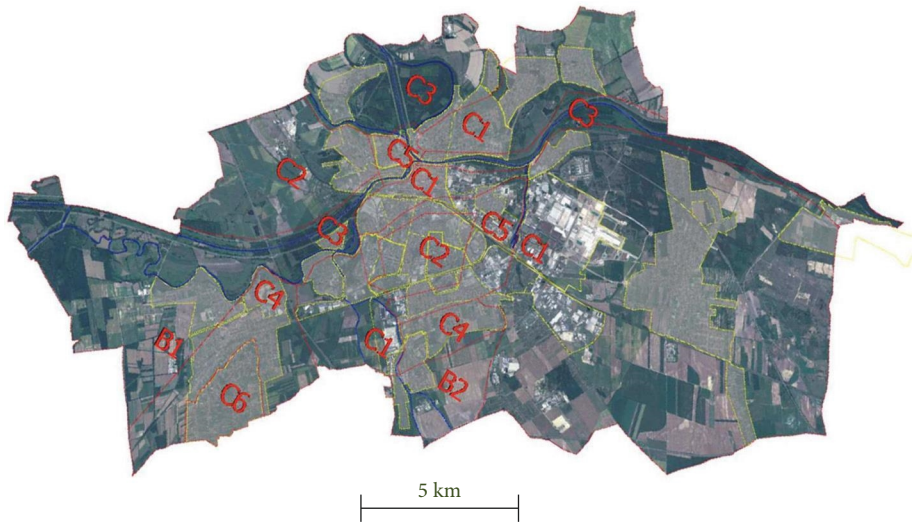

Figure 3: Microzonation map-based site soil properties of Győr [40].

acceleration on type C ground ($ag = \gamma_1.agR$), q of 1.5, which is the behavioral factor recommended for type 1 elastic response spectra (EN 1998-1).

4. Geometric and Material Properties of Building

A typical six-story structure of three equal floor heights measuring 40 m × 16 m in length and width, which adheres to Győr's building codes, was considered, remodeled, and analyzed according to Eurocode specifications. The plan drawings of the masonry and reinforced concrete (RC) buildings are shown in Figure 5. Members were carefully selected to replicate typical ground-level structures and to test their resilience against the local site spectra, considering two different material properties (masonry and reinforced concrete). The buildings were modeled and analyzed using AxisVM software, a finite element analysis tool. For the RC building, high-strength structural steel S460 with a concrete grade of M25 is considered, while for the masonry building, solid clay bricks of grade M2.5 G are considered, with the following typical and replicable dimensions provided below. The columns dimensions are 230 mm × 230 mm, the beam dimensions are 230 mm × 450 mm according to the effective depth ratio, the slab thickness is 175 mm, and the wall thicknesses are 230 mm. Additionally, the structure comprises a total of 39 columns. The masonry building features a monolithic, continuous length of walls. The imposed loading for the structure is considered to be an important building by utilizing the importance factors as multipliers to enhance the stability of the initial design loads, as specified in the building code to serve the purpose of ensuring life and safety following an earthquake.

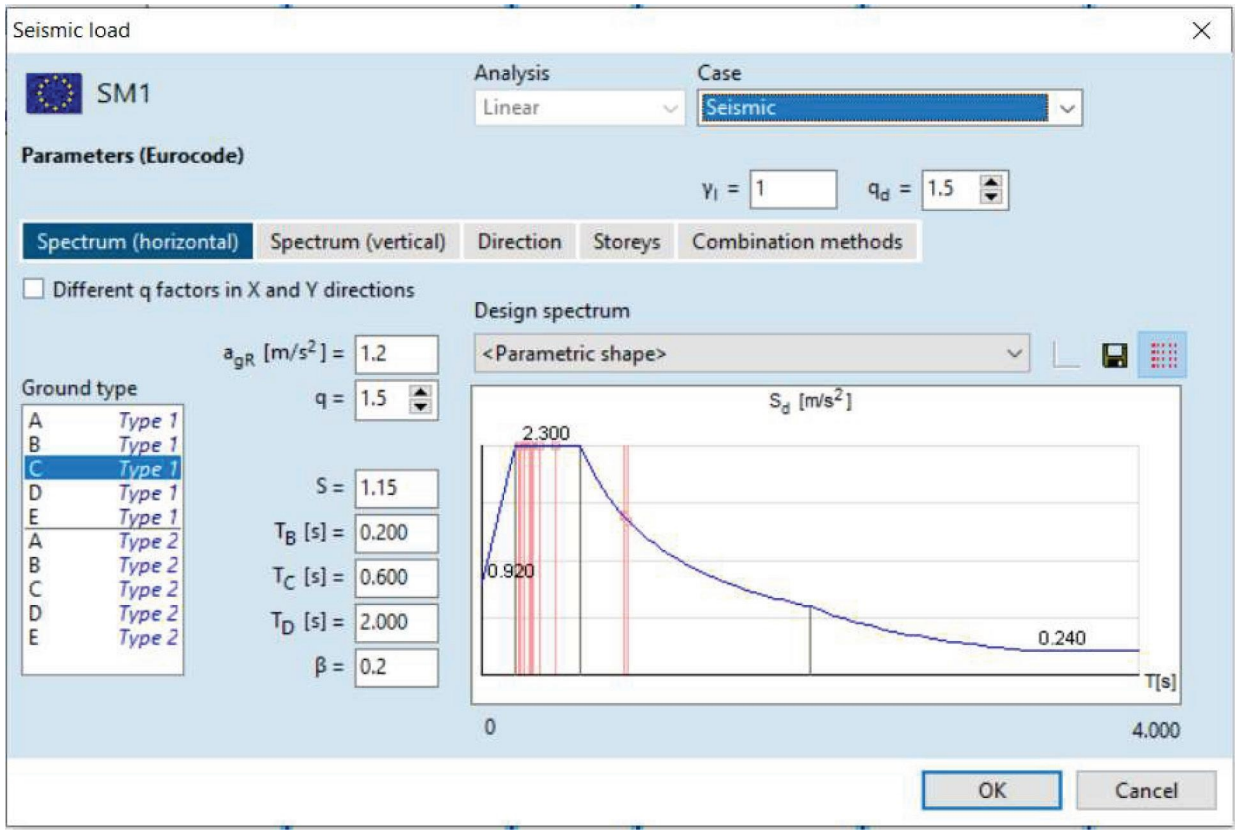

Figure 4: Seismic load indication in AXISVM software.

5. Results

This section provides a comprehensive analysis of the local site response, seismic analyses, and structural behavior of reinforced concrete and masonry buildings in Győr, Hungary, subjected to seismic forces. Initially, the local site response was investigated using the MASW method, revealing variations in soil properties across different profiles shown in Figure 6. The obtained shear wave velocity (V_s), unit weight, and exploration depth enhanced the seismic analysis output for the site amplifications through a one-dimensional response curve (local site-specific spectra). The REXEL software facilitated scenario-based assessment and scaling of earthquake records considering parameters such as near-fault distance, soil type, and PGA for records shown in Figure 7. The structural response of the RC and masonry buildings was evaluated using the AxisVM software, which highlights differences in displacements and stresses under elastic design- and site-specific spectra in Figure 8. Structural designs were scrutinized for their ability to withstand seismic forces, with proposed retrofitting strategies outlined for failed members shown in Figures 9 and 10, respectively.

5.1. Local Site Response Analyses. This research utilized the MASW method, a widely recognized nondestructive geophysical technique, to investigate the effect of subsoil layers considering the shear wave velocity profile of the subsurface on ground motion data from the bedrock to the ground surface. The three selected sites, from Győr Hungary, for this study were carefully chosen based on their specific geological and geophysical characteristics. The obtained shear wave velocity and soil properties data are summarized in Figure 6.

The corresponding diagram illustrating the shear wave velocity (V_s) profiles of the considered soil types is presented in Figure 11, depicting measurements up to a depth of 30 m below the ground surface.

To facilitate effective response analysis, REXEL was utilized for scenario-based assessment, which involved selecting and scaling ground motions, as well as conducting time response history analysis. Various parameters, including the near-fault distance, intensity, magnitude, soil type, PGA of 1.2 g specific to the study area (Győr, Hungary), and a return period of 475 years, were carefully considered and scaled. The targeted design response spectrum and the corresponding scaled site-specific response spectra are illustrated in Figure 7. The scaled ground motion data, the corresponding response spectra depicted in Figure 7, is used to consider the effect of soil properties on ground motion data through amplification.

These collected soil and scaled ground motion data were then analyzed using a computer software. STRATA performs equivalent linear site response analysis in the frequency domain and permits the randomization of the site characteristics such as the PGA transfer function and the local site acceleration spectra which represent the maximum ground acceleration experienced at a spot during the shaking of an

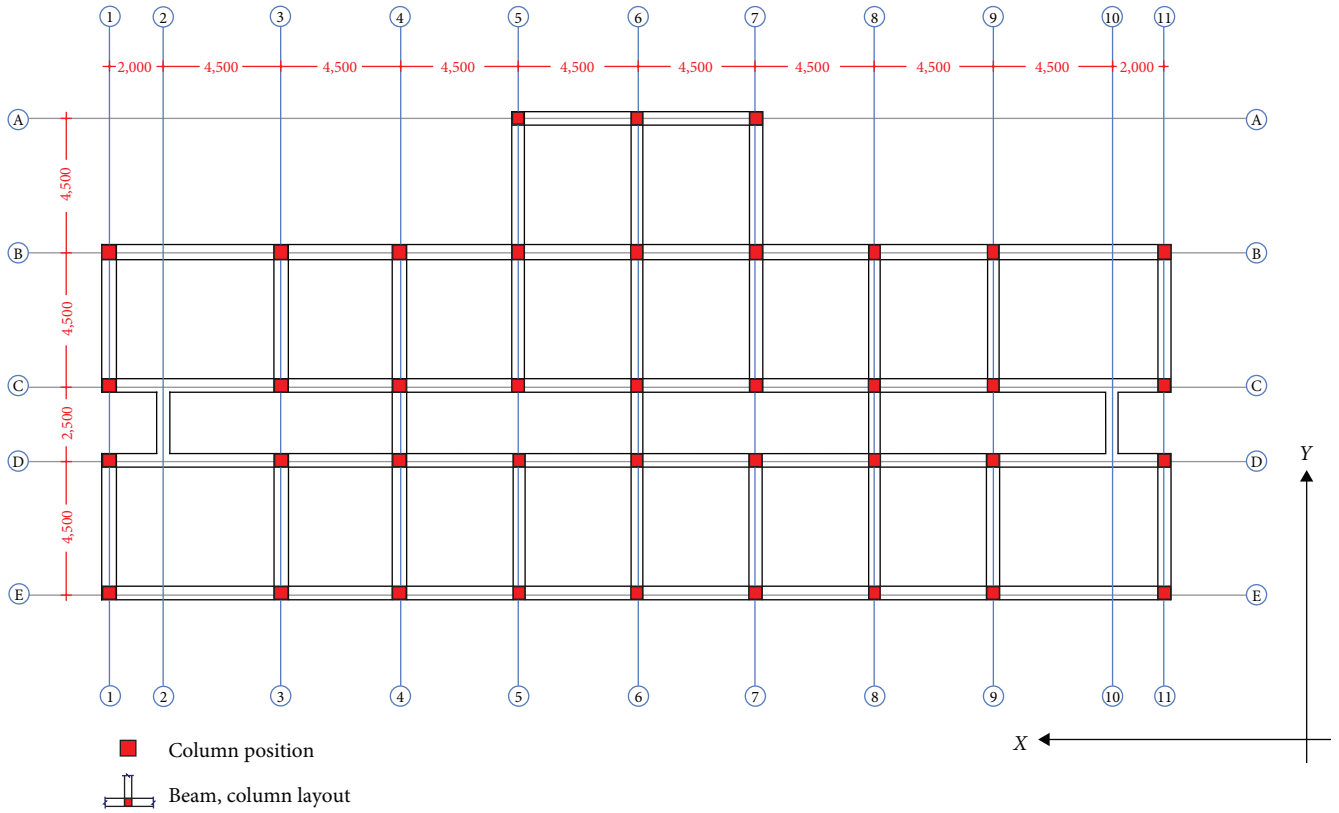

(a)

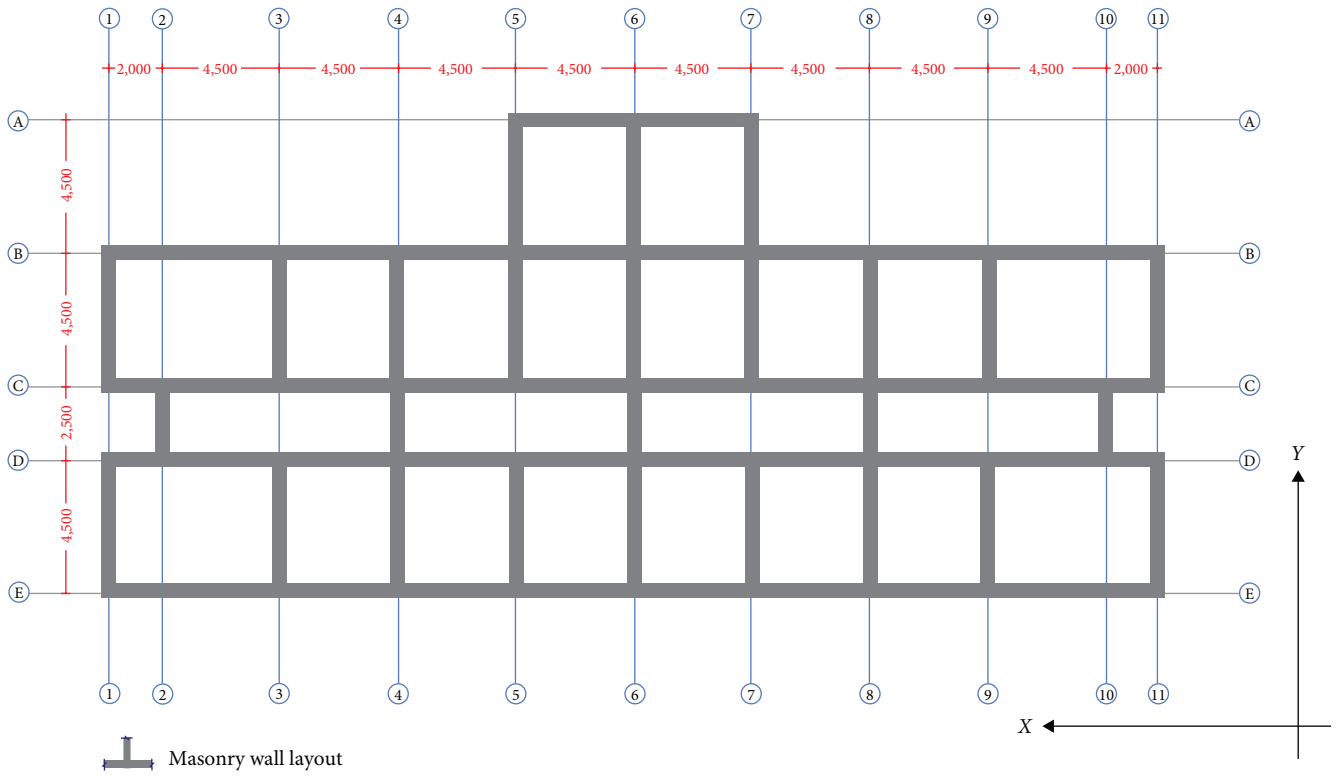

(b)

FIGURE 5: Plan drawings of (a) reinforced concrete and (b) masonry buildings.

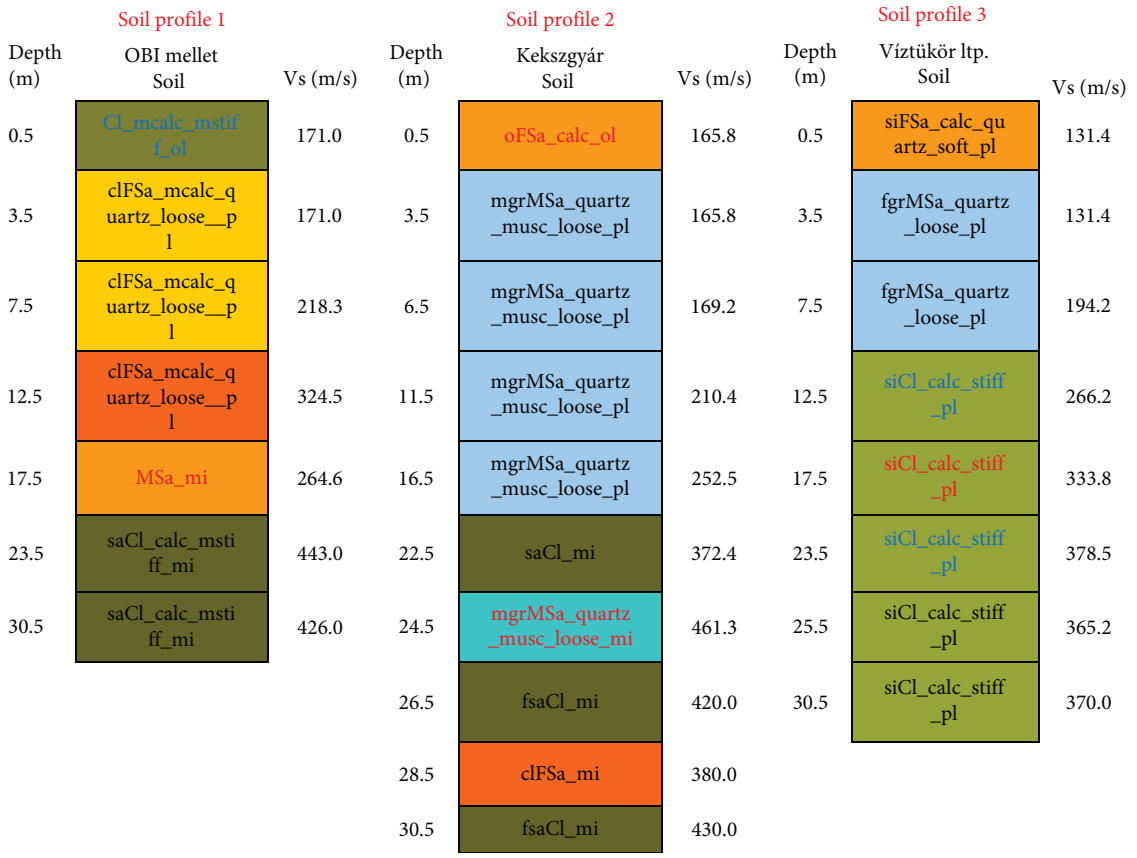

Figure 6: Soil profiles obtained at three different locations in Győr, Hungary.

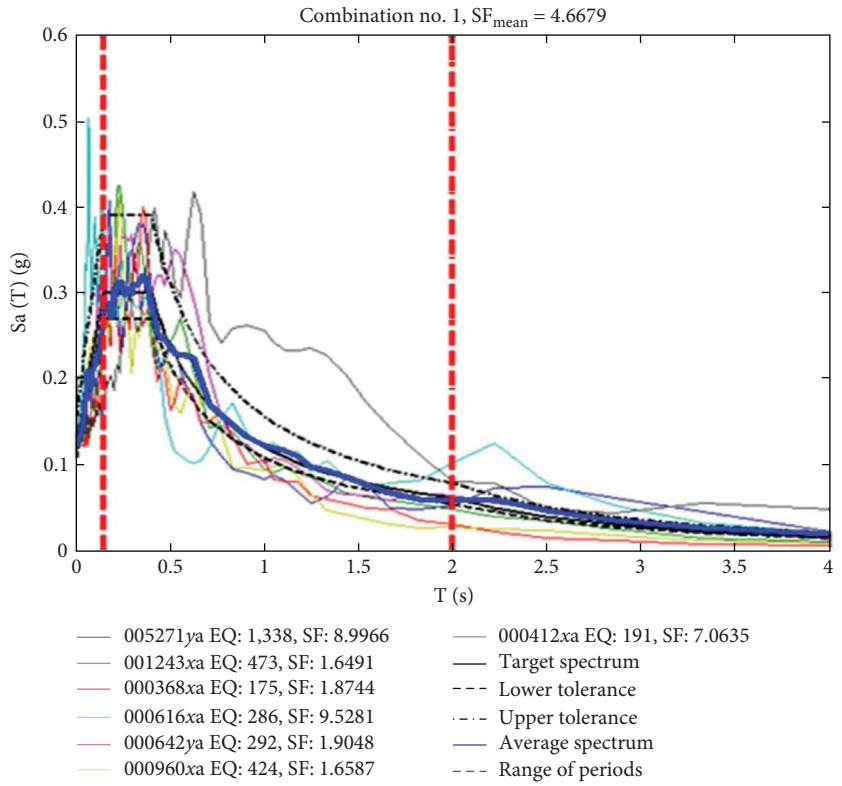

Figure 7: Design response spectrum and scaled site-specific response spectra [33].

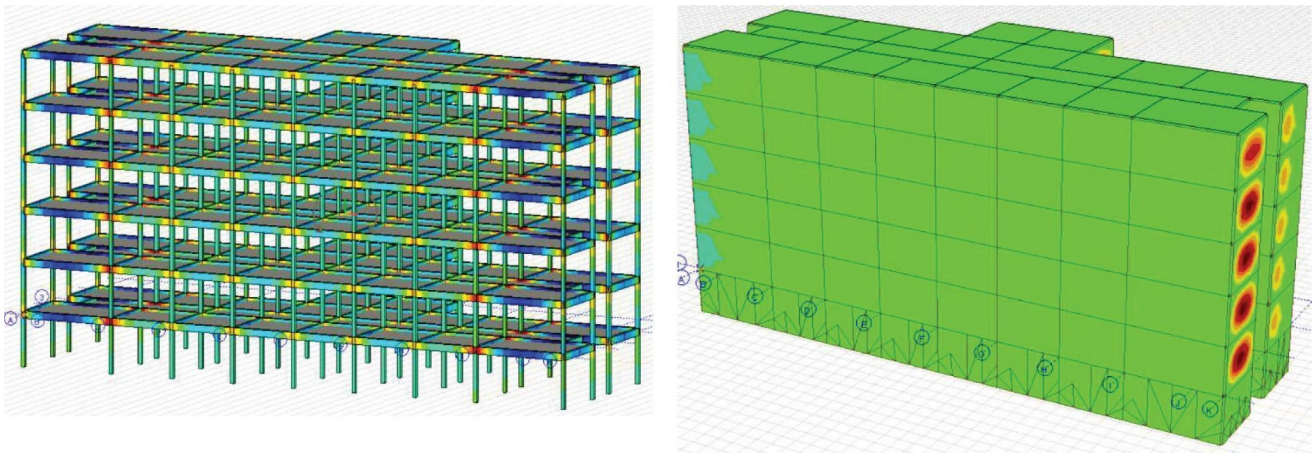

Figure 8: Layout and 3D model showing stresses due to dynamic loading for the reinforced concrete and masonry building.

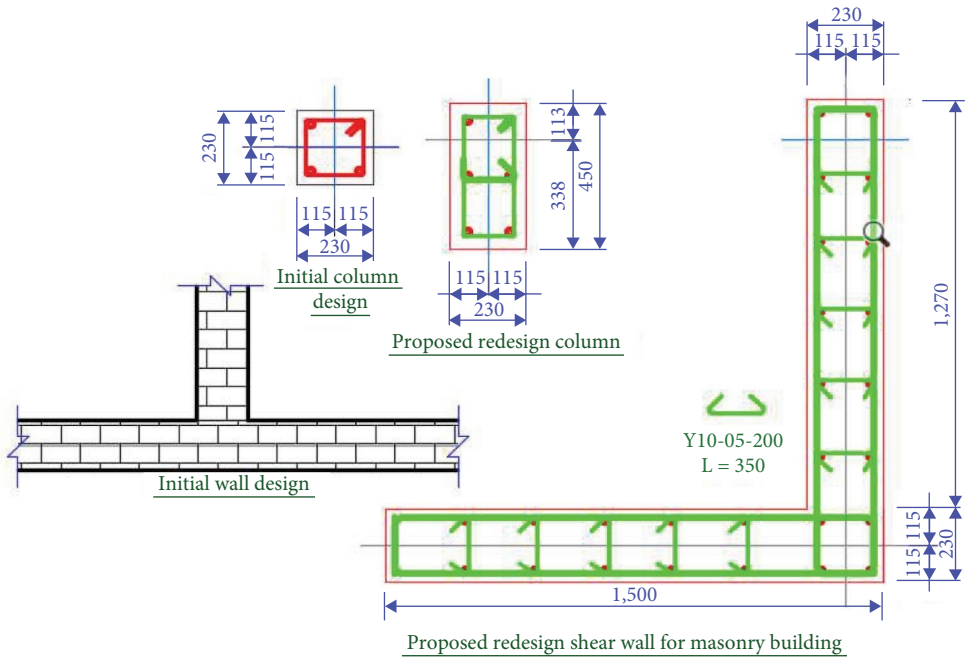

Figure 9: Proposed cross-sections for the retrofitting of columns and shear walls.

earthquake. The data in Figure 6 were input into the STRATA software, and the results of shear wave velocity (V_s), PGA, and site-specific spectrum were obtained as shown in Figures 11 and 12. For the analysis of the presented results after running 100 realizations for a 475-year return period, the findings indicate that the site location Kekszgyár (soil profile II) has the highest PGA and shear wave velocity among the preselected sites. This suggests that this site will experience the strongest ground shaking during an earthquake, with the PGA on the recording surface reaching 0.32 g, representing the maximum level of ground motion acceleration that can occur on the surface during seismic events and will be used in the design and analysis of buildings.

To assess the structural response to ground motion at the selected sites, the acceleration response spectrum was generated for each of the three locations, as shown in Figure 13. Figure 13 shows the relationship between the vibration frequency and the corresponding maximum and minimum accelerations experienced by the site obtained using the STRATA software. To evaluate the structural response to design standards, the resulting plot was compared with the type 1 and type 2 elastic response spectrum specified in Eurocode 8. From Figures 11, 12, and 13, the seismic assessment shows that soil profile II (Kekszgyár) has the highest site amplification, with 48% above type 1% and 23% above type 2 design spectra, respectively. These results obtained

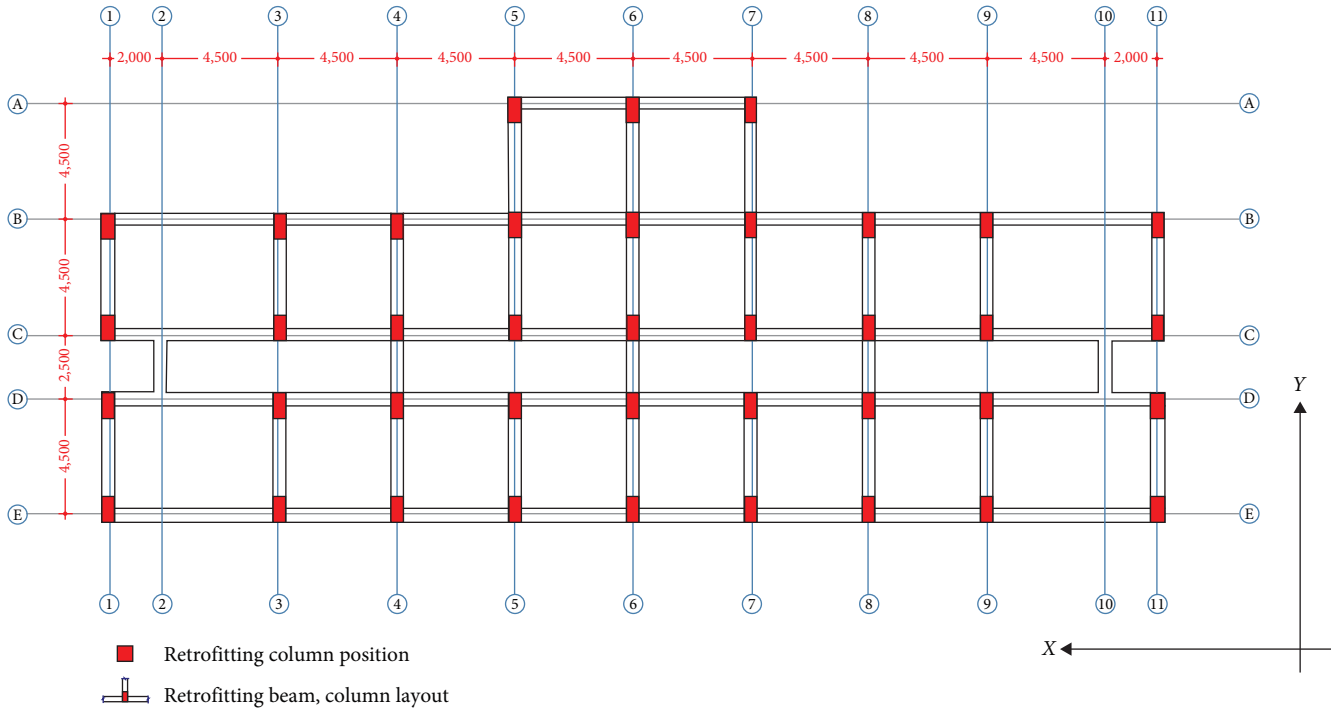

(a)

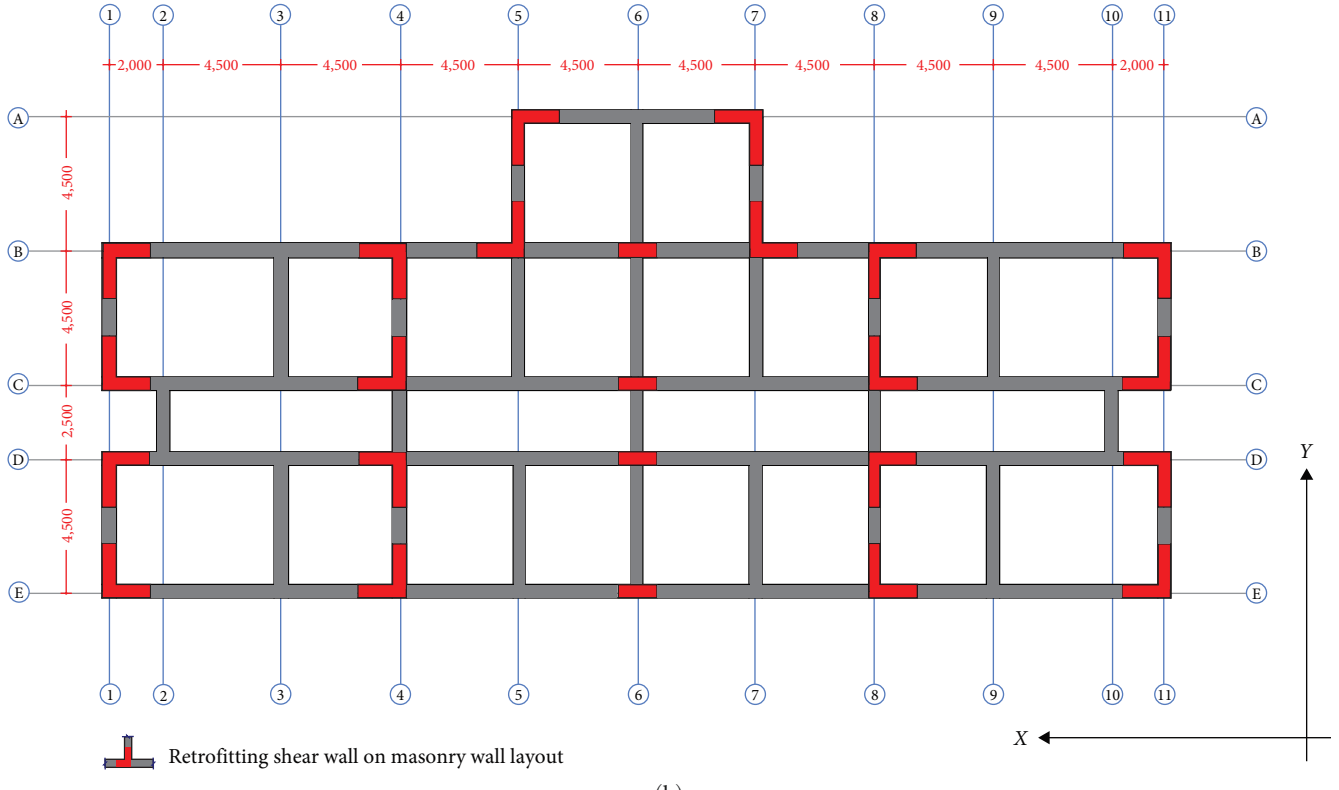

(b)

Figure 10: Position and layout of the columns and shear walls for the redesigned (a) reinforced concrete and (b) masonry buildings redesigned.

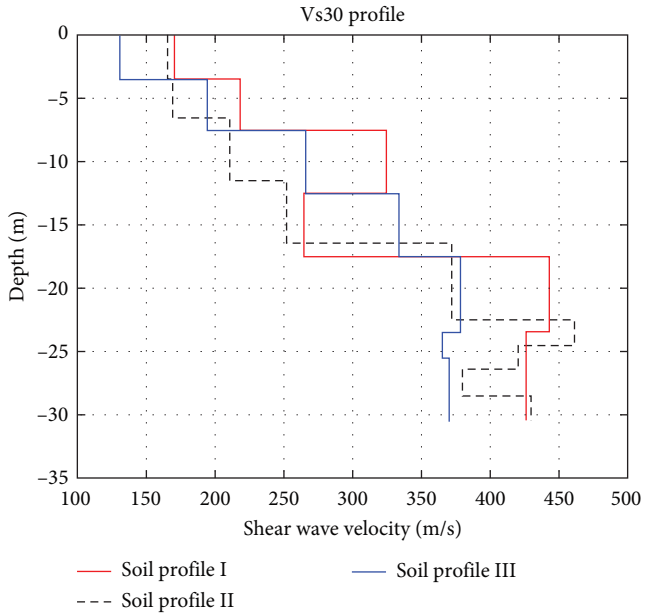

Figure 11: Shear wave velocity profiles for the three considered sites.

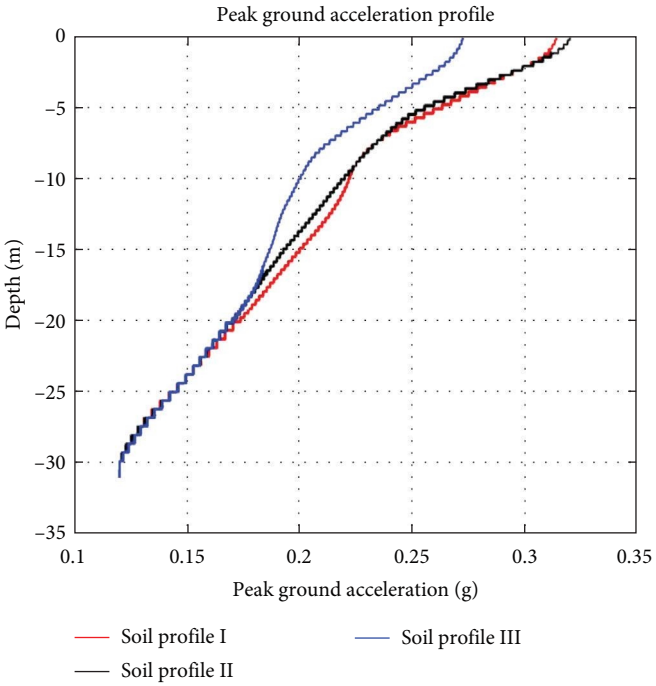

Figure 12: Peak ground acceleration (PGA) profiles for the three considered sites.

were used to assess the seismic performance of the RC and masonry buildings in AxisVM software.

5.2. Evaluating the Behavior of Modeled Buildings Using AxisVM Finite Element Software. The process of assessing the performance of buildings under the influence of seismic forces generated by soil properties is a systematic evaluation that involves subjecting building models to seismic stresses, followed by a

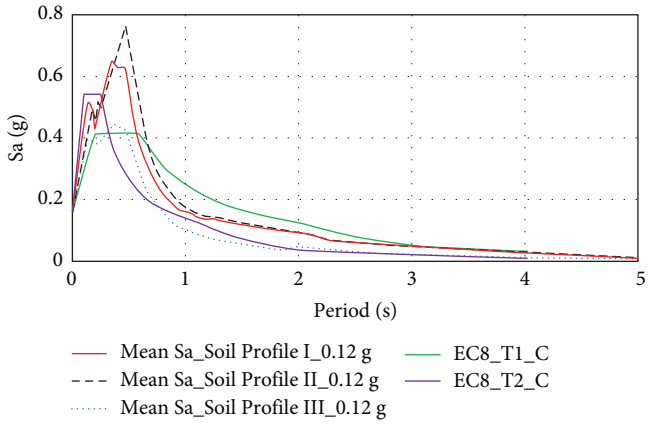

Figure 13: Comparison of type 1 and 2 elastic response spectra with the specific site acceleration spectrum profiles for the maximum and minimum soil type C profiles.

comprehensive analysis of standard seismic data and soil parameters. By collecting, analyzing, and comparing data against explicitly defined performance criteria, this approach equips designers with invaluable insights into how their designs perform during real-world usage [27]. The buildings were designed considering the design response spectrum compliant with Eurocode 8 standards, considering site seismicity (PGA = 0.12 g) and soil properties (soil type C). The linear and nonlinear geometric properties of the buildings were taken into account during the analysis. The corresponding stresses on the buildings resulting from the analyses are illustrated in Figure 8.

Furthermore, seismic analyses were performed to compute the displacements and stresses arising from the specified dynamic loading encompassing elastic design-specific and site-specific response accelerations as the response of buildings shown in Figures 14 and 15. The earthquake resistance capabilities were assessed by using the response spectrum in the weakest direction in coordinate Y on the grid 9–9 of the buildings as seen in the building plan in Figure 5. In the overall structural displacements of the reinforced concrete structure, the maximum displacement when the design spectrum was applied was 48.13 and 79.28 mm for the site-specific spectrum, respectively, showing a clear difference of 31.15 mm. This difference results in the variation between the design spectrum and the site-specific spectrum based on the soil properties and its corresponding ground amplification as shown in Figure 14.

In the overall masonry building displacements, the maximum displacement when the design spectrum was applied is 91.409 and 162.582 mm for the site-specific spectrum, respectively, showing a clear difference of 71.173 mm more than reinforced building by 38.762 mm. This difference results in the variation between the design spectrum and the site-specific spectrum based on the soil properties and its corresponding ground amplifications as shown in Figure 15.

To understand the collapse and deflection behavior of these structures under seismic forces, the collapse mechanisms of the reinforced and masonry buildings are considered and presented in a graphical format, as shown in Figure 16. In terms of overall structural displacements, the RC structure

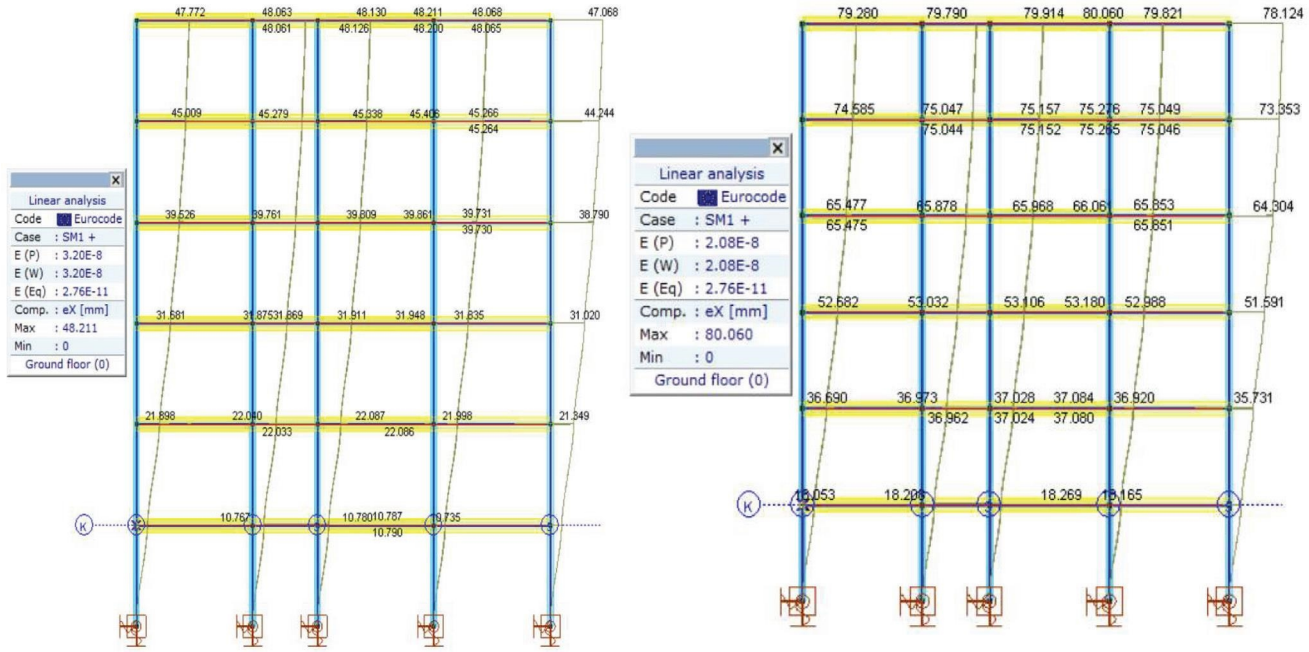

Figure 14: Reinforced concrete horizontal structural performance-based displacement for elastic design- and site-specific spectrum.

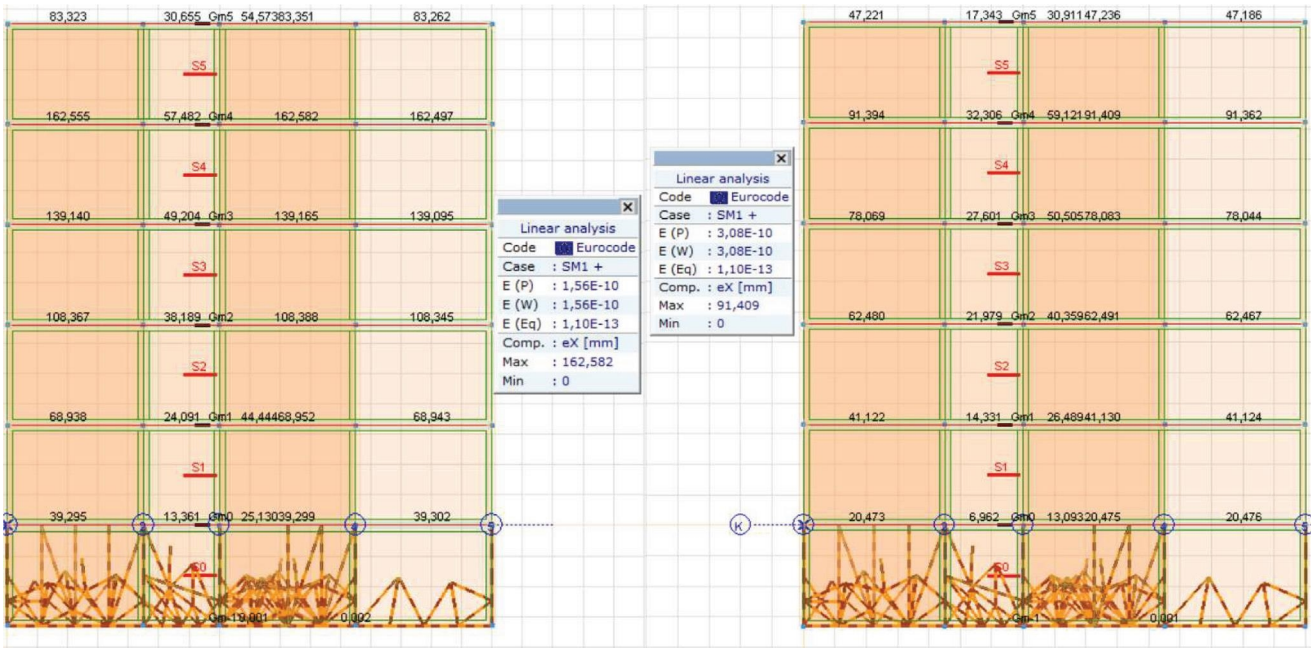

Figure 15: The horizontal structural performance-based displacement of the mason for the elastic design- and the site-specific spectrum.

exhibited a maximum displacement of 48.13 and 79.28 mm for the design- and site-specific spectra, respectively, showcasing a difference of 31.15 mm. Conversely, the masonry building displayed larger displacements, with maximum values of 91.409 and 162.582 mm for the design- and site-specific spectra, respectively, indicating a difference of 71.173 mm. Additionally, when compared to the RC building, the masonry structure experienced a greater displacement difference between the design- and the site-specific spectra, highlighting the influence of soil properties and high-ground amplification on the observed local site-specific spectra.

5.3. Effectiveness of Structural Designs in AxisVM for Seismic Response Analysis. Based on EN 1998-1:2004 (E), the design method for every element of the structural system should be chosen, carefully designed, and detailed for energy dissipation

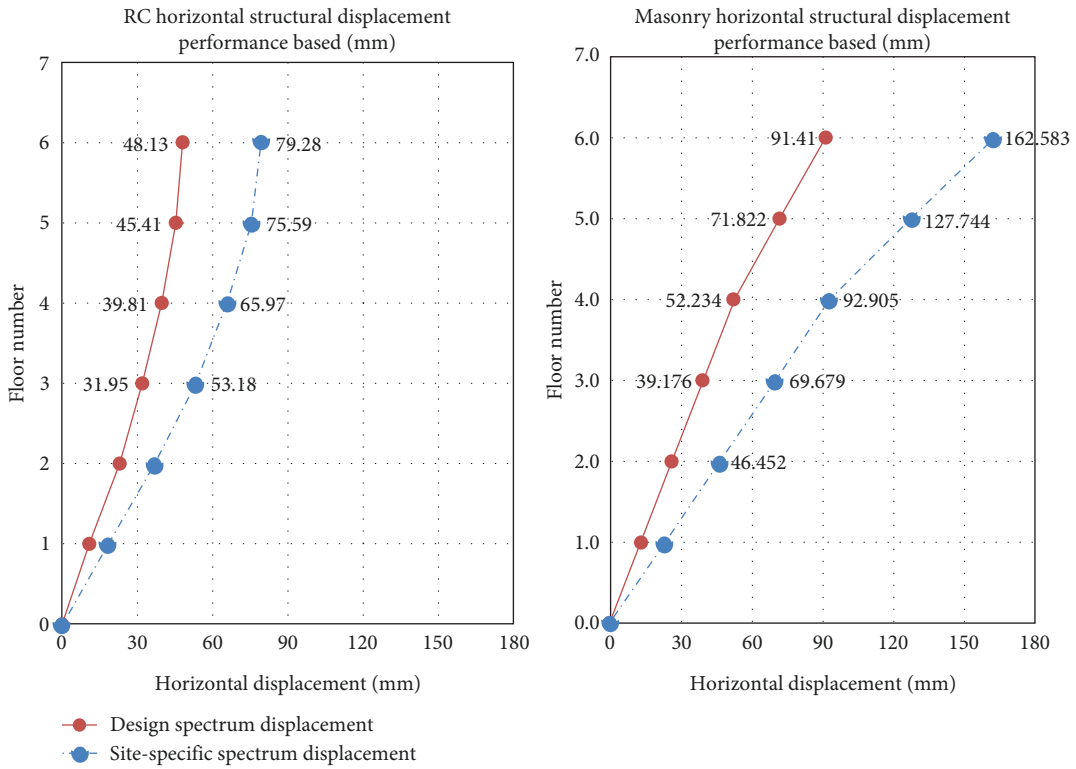

FIGURE 16: RC and masonry horizontal displacement curve when elastic design- and site-specific spectrum are applied.

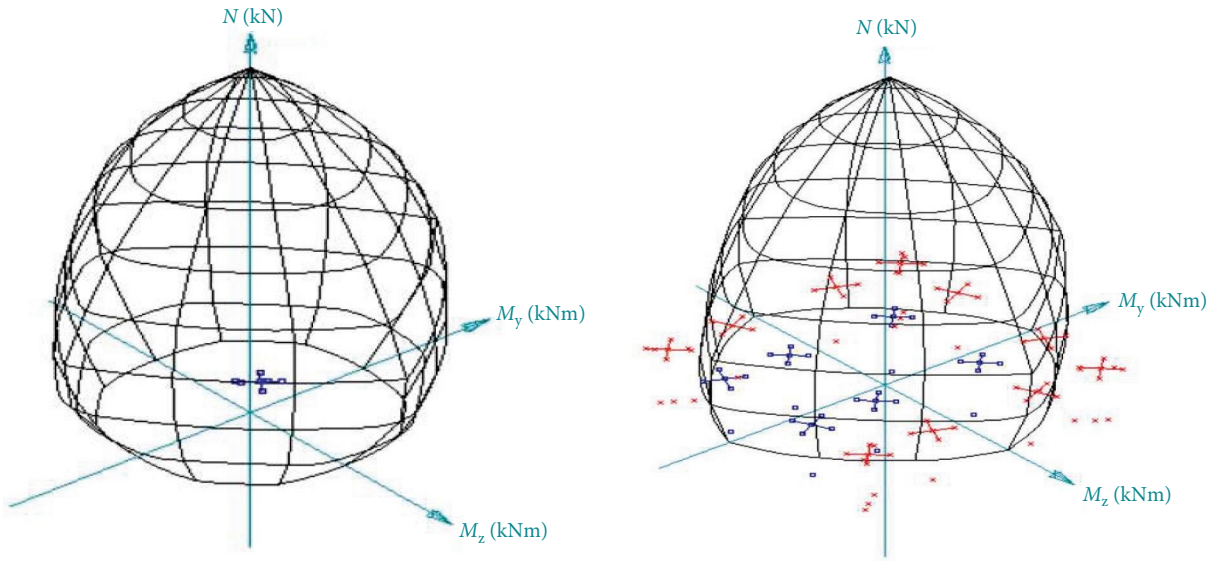

FIGURE 17: The distortion diagrams show the column-carrying capacity for the elastic design spectrum and the site-specific spectrum exceeding its capacity by showing red patches.

under severe deformations, and providing other structural elements with sufficient strength so that energy dissipation can be maintained to prevent damage and collapse by seismic actions. To unravel the effectiveness of structural designs for the design- and site-specific response in AxisVM, member elements are compared to the conventional capacity design in terms of failure and the ability to withstand seismic forces applied by ensuring that the applied load on a column does not exceed its capacity to withstand that load. For the reinforced structure, when the site-specific response spectra obtained from STRATA were applied, all columns were observed to be exceeded by failing to satisfy the condition to resist the applied force and moment, as shown in equation (1) and Figure 17.

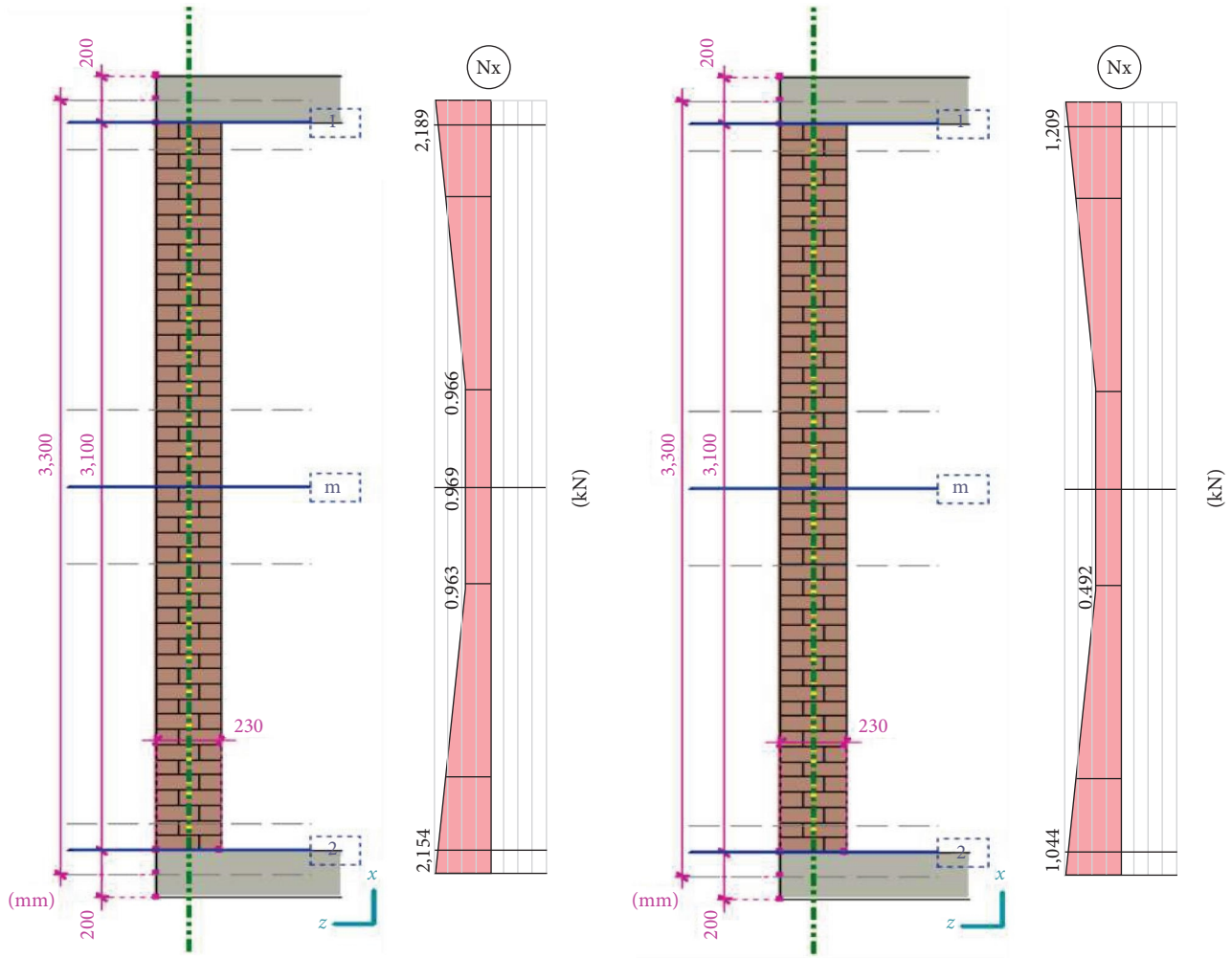

FIGURE 18: Horizontal displacement of solid brick members results in tension instead of compression causing failure of members.

$$\eta N = \frac{N_{Ed}}{N_{Rd}} < 1, \tag{1}$$

where ηN is the utilization ratio or factor that enhances a check to ensure that the utilization ratio remains less than 1 to guarantee the structural integrity and safety of the column under the expected loads. N_{Ed} is the design load on the column, and N_{Rd} is the resistant load on the column, respectively.

In the case of design spectra, $\eta N = 0.1729$, which is less than 1 and has satisfied the condition according to EC2, EN: 3.1.6, 1992, and $\eta N = 1.464$, which is greater than 1.

Similarly, the case of the masonry building was also checked in terms of capacity and its ability to bear the loading from the structure using elastic design- and site-specific spectra. The results show the inability of the walls to resist seismic forces for both spectra, resulting in excessive deflection pulling the members from compression to tension, as shown in Figure 18.

5.4. Proposed Retrofitting or New Design Method. As shown in Figure 12, there has been significant horizontal deformation, resulting in a substantial variance of 31.15 mm (48.84%) for the reinforced concrete building and 71.173 mm (55.79%) for the masonry building. These deformations have led to the failure of columns and walls under the given loading conditions. Consequently, it is observed that the column capacities exceed the design capacity, as illustrated by the utilization ratio (ηN) being greater than 1. The column's load-carrying capacity for the site-specific spectrum exceeds its capacity, indicating the presence of a red patch in Figure 17. Therefore, the following redesign technologies were applied to the failed members, in the case of columns for the reinforced structure, the selection of columns is the most ideal and has proven in the remodeled building that columns of dimensions 230×450 mm can withstand and resist shock forces, while shear walls were applied at the major corners of the bricks (masonry) to act as a resistance to the seismic forces in Figures 9 and 10.

The columns and walls for the redesigned reinforced and masonry buildings redesigned to limit deformation and damage to the structure, allowing it to withstand seismic forces, are shown plan view of buildings in Figure 10.

Compared to the initial deformations in the reinforced and masonry buildings, there has been a notable reduction in

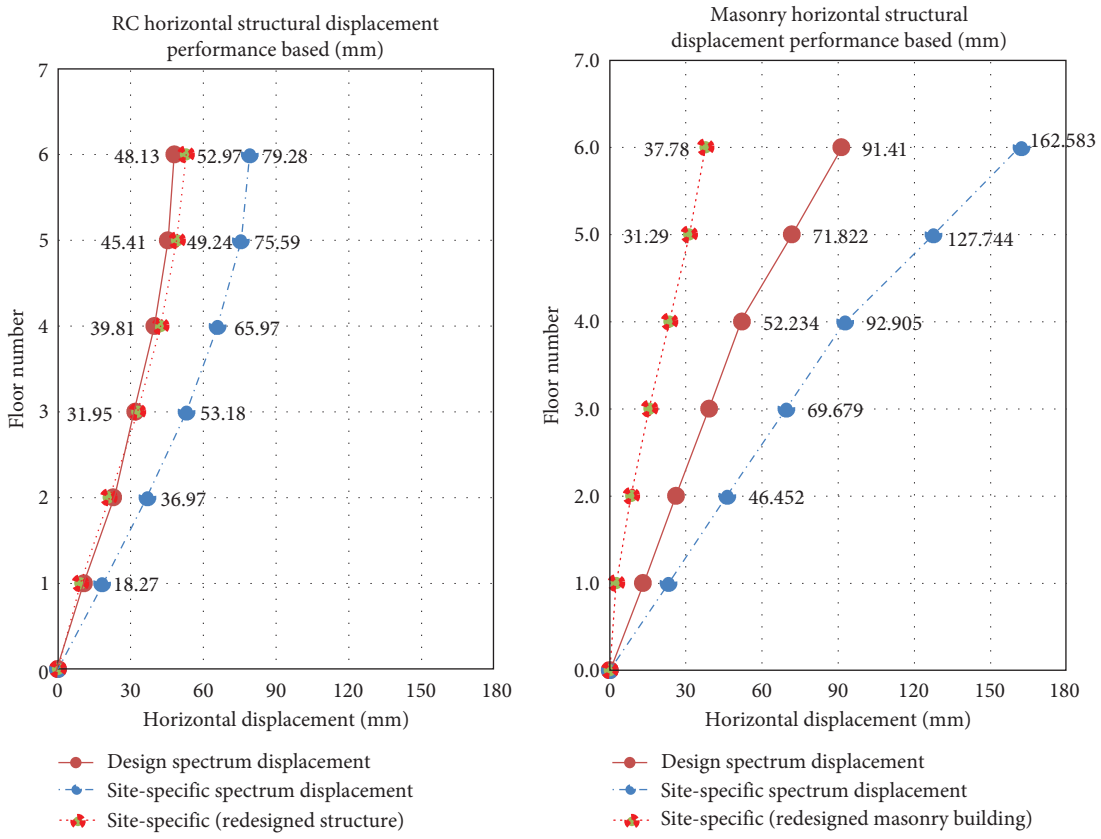

Figure 19: Comparative assessment of the deflection performance for the retrofitted buildings.

Table 2: Life cycle assessment focusing on exceeded elements in the reinforced concrete building.

Indicators (parameters)	Ecocosts (€)	Carbon footprint (kg) CO_2 eq.
Steel rebar (reinforcement)	1,535.82	6,801.50
Cement	639.51	3,385.64
Sand	4.51	17.30
Crushed aggregates	33.05	120.17
Transportation	8.54	30.97
Electricity and gas	79.64	480.75
Total	2,301.07	10,836.33

structural deformation, with a decrease of 66.81% for the reinforced building and 100% for the masonry building since the retrofitted designs were adequately reinforced to withstand bending and twisting forces that exceeded their capacity when site-specific spectra were applied. These methods of retrofitting shows less compression or stretching without losing its original shape. It is worth noting that a stiffer structure deforms less under seismic and external loading, which is the case as seen in Figure 19.

6. Comparative Life Cycle Cost Assessment

To determine the most suitable and sustainable redesign technique while reducing environmental impact, retrofitted building members (columns and walls) undergo a life cycle analysis (LCA). Environmental impact assessments are performed using IdematLCA and OpenLCA in terms of ecological costs and carbon footprints. This analysis considers key indicators and major compositions of elements, such as the total volume of steel rebars and concrete required, to effectively determine ecocost and carbon footprint in terms of resource depletion, ecotoxicity, and human health. Tables 2 and 3 provide detailed information on these aspects. The total ecocosts and carbon footprint associated with the retrofitting process, considering factors such as steel rebar, cement, sand, crushed aggregates, transportation, and electricity and gas, amount to €2,301.07 and 10,836.33 kg CO_2 eq., respectively.

The table presents the results of a life cycle assessment focusing on the masonry building's retrofitting. It outlines various indicators (parameters), such as ecocosts (in euros) and carbon footprint (in kilograms of CO_2 equivalent), associated with different elements involved in the retrofitting

Table 3: Lifecycle assessment of retrofitting the masonry building.

Indicators (parameters)	Ecocosts (€)	Carbon footprint (kg) CO_2 eq.
Steel rebar (reinforcement)	1,286.41	5,696.98
Cement	773.73	4,096.22
Sand	5.46	20.94
Crushed aggregates	39.98	145.39
Transportation	9.51	34.47
Electricity and gas	72.73	439.06
Total	2,187.83	10,433.05

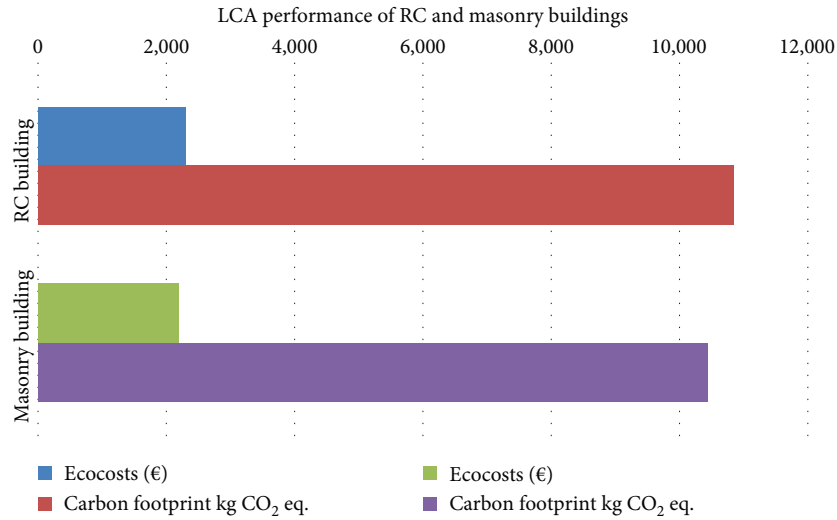

Figure 20: Difference in life cycle assessment performance of retrofitting the considered buildings with their level of environmental pollution and material depletion effects.

process. These elements include steel rebar (reinforcement), cement, sand, crushed aggregates, transportation, and electricity and gas, as illustrated in Table 2. The total ecocosts and carbon footprint for the retrofitting of the masonry building are calculated as €2,187.83 and 10,433.05 kg CO_2 eq., respectively.

The environmental impact performance of the proposed retrofitted members is presented graphically in Figure 20. The change in CO_2 emissions from the retrofit of the RC building to the masonry building resulted in a decrease of 403.28 kg CO_2 eq, while the ecocost decreased by €113.24. The results indicate that reinforcing the masonry building is less costly compared to reinforcing the reinforced concrete building in this particular case study.

To better understand the breakdown of the individual contributions of the failed elements in terms of ecological cost and carbon footprints by various key indicators, a modal split is considered as shown in Figures 21 and 22 for reinforced concrete and masonry structures, respectively. In the life cycle assessment of the reinforced concrete building (Figure 21), the proportions of various indicators in terms of ecocosts and carbon footprint are as follows: Steel rebar (reinforcement) accounts for 66.69% of the ecocosts and 62.75% of the carbon footprint, while cement contributes 27.77% to the ecocosts and 31.23% to the carbon footprint. Sand represents a minimal portion, contributing 0.20% to the ecocosts and 0.16% to the carbon footprint, followed by crushed aggregates with 1.44% of the ecocosts and 1.11% of the carbon footprint. Transportation and electricity and gas make relatively smaller contributions, representing 0.37% and 3.46% of the ecocosts and 0.29% and 4.46% of the carbon footprint, respectively.

The following are the proportions of different indicators in terms of ecocosts and carbon footprint in the life cycle assessment of the masonry building (Table 3): Cement makes up 35.36% of the ecocosts and 39.28% of the carbon footprint, while steel rebar (reinforcement) makes up 58.76% of the ecocosts and 54.61% of the carbon footprint. Crushed aggregates come in second with 1.83% of the ecocosts and 1.39% of the carbon footprint, while sand makes up the smallest portion at 0.25% of the ecocosts and 0.20% of the carbon footprint. Relatively speaking, transportation, gas, and electricity and costs account for 0.43% and 3.33% of the environmental costs and 0.33% and 4.23% of the carbon footprint, respectively.

The results in Figures 21 and 22 show that the equivalent carbon footprint generated is mainly dominated by steel reinforcement, which has a total carbon footprint per kilogram greater than 50%. This is followed by cement, which has a carbon equivalent emission per kilogram above 35%,

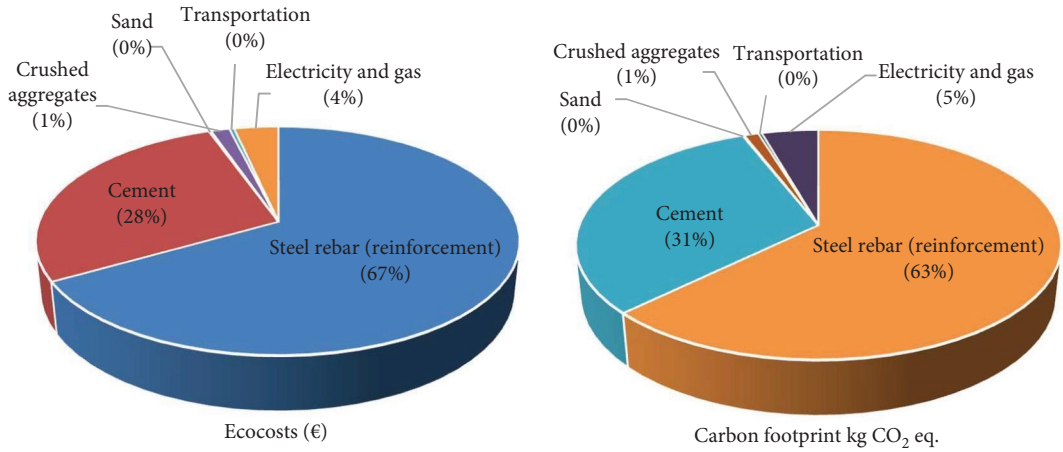

Figure 21: The ecological cost and equivalent carbon footprint (CO_2) of retrofitting the reinforced concrete building show the percentage contribution of each indicator and parameter.

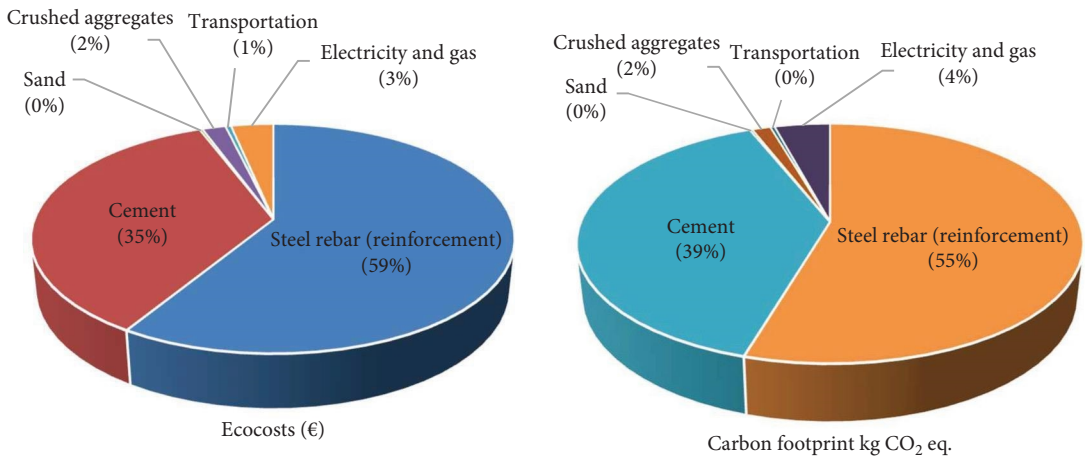

Figure 22: The ecological cost and equivalent carbon footprint (CO_2) of the masonry building shows the percentage contribution of each indicator and parameter.

which is also a major constituent of concrete and, of course, also has a higher percentage of environmental impact in surrounding areas and production factors. In terms of ecological cost comparison, the difference in the cost of stabilizing and preventing the effect of environmental pollution is negligible, with a difference of €113.24 coming mainly from the ecocosting of the masonry building, which implies that reinforced concrete buildings are better performed in seismic-prone areas since they can withstand more forces as seen in the results of the research and are less cost-effective in repairing damage than the masonry building since it will still bounce back to repairs that will have to do with reinforcing members with concrete and rebars to partially replace the brick walls.

7. Discussion

Earthquake records were generated for a return period of 475 years, considering a PGA of 0.12 g for Győr, Hungary, where the soil profiles were explored. The results obtained from STRATA after running 100 realizations for each profile show significantly higher surface amplification when compared to the types 1 and 2 elastic design spectra based on soil type C. The soil profile 2 site (Kekszgyár) has the highest surface ground motion amplification. These amplifications, considering the highest local spectral values (Kekszgyár), were fed into the AxisVM software, a finite element software used for structural design, taking into account two different building types (unreinforced masonry and reinforced concrete structures) for a six-story building based on Eurocodes 8, 7, and 2. These buildings were designed using the determined site-specific acceleration response spectrum from STRATA (a one-dimensional response software) to study the effects of site and design responses for those buildings. The results from AxisVM show that the overall structural displacements of the RC and masonry building structures exceeded the designed capacities when the local site spectra were applied. In the first place, the RC building was able to withstand the elastic design spectrum forces, whereas the masonry building failed by causing all the wall joints to sway, resulting in tension rather than

compression. Relatively, in the masonry building, walls designed according to Eurocodes 7 and 8 were observed to have sheared into multiple zones, causing the entire top and bottom joints to be in tension instead of compression, exceeding the capacity, and hence resulting in total failure. In the reinforced structure, the members were able to withstand the loads and seismic forces at the design spectrum specified in Eurocode 8 under type C. When considering the local spectra for the reinforced design, it was observed that all columns supporting the structure produced a greater deflection, causing all columns to exceed the designed capacity, resulting in failure as well. Considering all these factors, a concise decision based on the results obtained is reached to provide specifications to strengthen the failed members by proposing redesigned methods of increasing the member stiffness. Based on the proposed retrofitting methods, there was a significant reduction in horizontal deflection from 97.28 to 52.97 mm for the RC building and from 162.58 to 37.78 mm, respectively. The results show no significant changes in the ecocost and carbon footprint of the proposed retrofitting method.

8. Conclusions

In this study, six-story reinforced concrete and masonry buildings from Győr, Hungary, were initially designed according todesign spectra, with the site's PGA of 0.12 g and soil properties categorized as soil type C. Subsequently, they (reinforced concrete and masonry buildings) were evaluated to determine the impact of site soil properties on seismic load amplification. Strengthening measures were then implemented to ensure their ability to withstand seismic loads effectively. Finally, the redesign process and its environmental impact were examined, revealing the following findings:

(i) The determined site-specific response spectra have been seen higher than the Eurocode-specified elastic design spectra with 48% above type 1% and 23% above type 2 design spectra, respectively, considered for specific locations and upper shear wave velocity (V_{s30}).

(ii) When the site-specific response spectrum is considered for the analysis of buildings, the load-carrying elements (e.g., columns, walls) have exceeded in all cases.

(iii) Retrofitting failed members resulted in a significant reduction in deflection, highlighting the effectiveness of customized retrofitting strategies in improving structural resilience.

(iv) In terms of the performance of buildings, the RC building has shown more resistance to seismic forces by yielding less deflection of less than 2 inches as compared to the masonry building when the local site-specific spectra considered causing a whooping of over 4 inches in deflection resulting to a total failure.

(v) The environmental impact assessment of retrofitted failed members for both building types reveals no significant difference in terms of ecocost and carbon footprint, primarily attributable to the chosen retrofitting method. Interestingly, results for the retrofitting of the RC building to the masonry building resulted in a decrease of 403.28 kg CO_2 eq. in CO_2 emissions and a reduction of €113.24 in ecocost.

However, a notable limitation of this research emerged concerning the use and methods of retrofitting proposed to reduce horizontal deformations and to increase the member stiffness in the structures under consideration. The environmental impact assessments do not reveal significant changes in ecological costs and carbon footprints due to the proposed retrofitting method. Finally, future research should investigate site-specific design considerations for seismically prone areas, going beyond Eurocode 8 specifications. The impact of building height on masonry construction in seismic zones should be investigated, particularly in terms of reinforcement techniques for taller structures. Incorporating a range of building typologies and varying numbers of stories is essential to comprehensively assess the sustainability impact of strengthening interventions. Additionally, evaluating the environmental impact of construction methods and materials is critical to promoting sustainable practices. These investigations will improve the resilience and sustainability of buildings in earthquake-prone areas.

In conclusion, based on this investigation, reinforced buildings demonstrate a significant advantage in high seismic zones, showcasing greater resilience during peak response periods compared to masonry buildings. However, it is important to note that this conclusion is drawn from the findings of this study alone. Further investigation involving a wider range of buildings is necessary to validate and refine these findings.

Abbreviations

MASW:	Multichannel surface wave
PGA:	Peak ground acceleration
SSI:	Soil–structure interactions
RC:	Reinforced concrete
EERI:	Earthquake Engineering Research Institute
GEER:	Geotechnical Extreme Events Reconnaissance
EUCENTRE:	European Centre for Training and Research in Earthquake Engineering
TMDs:	Tuned mass dampers
SAmp:	Site amplification
SCT:	Seismic classifier toolbox
GHG:	Greenhouse gas
RVT:	Random vibration theory
q:	Soil behavioral factor
ηN:	Utilization ratio
NEd:	Design load on the column
NRd:	Resistant load on the column
CO_2 eq:	Equivalent carbon footprint emission
LCA:	Life cycle analysis
EC8_T1_C:	Eurocode 8 type 1 spectrum on soil type C
EC8_T2_C:	Eurocode 8 type 2 spectrum on soil type C.

Data Availability

Availability of data will be on request.

Conflicts of Interest

There is no conflict of interest in any part or section of the paper, being in data, results obtained, and conclusions, etc.

Authors' Contributions

Conceptualization is done by Benjamin Labar, Nurullah Bekta, and Orsolya Kegyes-Brassai; methodology by Benjamin Labar, Nurullah Bekta, and Orsolya Kegyes-Brassai; software by Benjamin Labar; validation by Benjamin Labar; formal analysis by Benjamin Labar, Nurullah Bekta, and Orsolya Kegyes-Brassai; investigation by Benjamin Labar, Nurullah Bekta, and Orsolya Kegyes-Brassai; resources by Benjamin Labar and Orsolya Kegyes-Brassai; data curation by Benjamin Labar; writing—original draft preparation, by Benjamin Labar and Nurullah Bekta; writing—review and editing, by Benjamin Labar and Nurullah Bekta; visualization by Benjamin Labar; and supervision by Nurullah Bekta and Orsolya Kegyes-Brassai.

References

[1] B. S. Bakir, H. Sucuoglu, and T. Yilmaz, "An overview of local site effects and the associated building damage in Adapazari during the 17 August 1999 Izmit earthquake," *Bulletin of the Seismological Society of America*, vol. 92, no. 1, pp. 509–526, 2002.

[2] A. F. Genç, E. E. Atmaca, M. Günaydin, A. C. Altunişik, and B. Sevim, "Evaluation of soil structure interaction effects on structural performance of historical masonry buildings considering earthquake input models," *Engineering Structures*, vol. 54, pp. 869–889, 2023.

[3] S. S. Tezcan, E. Kaya, İ. E. Bal, and Z. Özdemir, "Seismic amplification at Avcılar, Istanbul," *Engineering Structures*, vol. 24, no. 5, pp. 661–667, 2002.

[4] M. T. A. Chaudhary, "A study on sensitivity of seismic site amplification factors to site conditions for bridges," *Bulletin of the New Zealand Society for Earthquake Engineering*, vol. 51, no. 4, pp. 197–211, 2018.

[5] P. Karki, S. Pyakurel, and K. Utkarsh, "Seismic performance evaluation of masonry infill R.C. frame considering soil-structure interaction," *Innovative Infrastructure Solutions*, vol. 8, no. 1, pp. 1–15, 2023.

[6] A. Liratzakis and Y. Tsompanakis, "Impact of soil saturation level on the dynamic response of masonry buildings," *Frontiers in Built Environment*, vol. 4, Article ID 24, 2018.

[7] H. Matinmanesh and M. Saleh Asheghabadi, "Seismic analysis on soil-structure interaction of buildings over sandy soil," *Procedia Engineering*, vol. 14, pp. 1737–1743, 2011.

[8] A. M. E. Mohamed, H. E. Abdel Hafiez, and M. A. Taha, "Estimating the near-surface site response to mitigate earthquake disasters at the October 6th city, Egypt, using HVSR and seismic techniques," *NRIAG Journal of Astronomy and Geophysics*, vol. 2, no. 1, pp. 146–165, 2019.

[9] D. Pitilakis and C. Petridis, "Fragility curves for existing reinforced concrete buildings, including soil-structure interaction and site amplification effects," *Engineering Structures*, vol. 269, Article ID 114733, 2022.

[10] A. Brunelli, F. de Silva, A. Piro et al., "Numerical simulation of the seismic response and soil-structure interaction for a monitored masonry school building damaged by the 2016 Central Italy earthquake," *Bulletin of Earthquake Engineering*, vol. 19, no. 2, pp. 1181–1211, 2021.

[11] Ö. C. Özdağ, T. Gönenç, and M. Akgün, "Dynamic amplification factor concept of soil layers: a case study in İzmir (Western Anatolia)," *Arabian Journal of Geosciences*, vol. 8, no. 11, pp. 10093–10104, 2015.

[12] J. D. Pettinga and M. J. N. Priestley, "Dynamic behaviour of reinforced concrete frames designed with direct displacement-based design. European school of advanced studies in reduction of seismic risks," *Journal of Earthquake Engineering*, vol. 9, no. sup2, 2010.

[13] S. M. Bijukchhen, N. Takai, M. Shigefuji, M. Ichiyanagi, T. Sasatani, and Y. Sugimura, "Estimation of 1-D velocity models beneath strong-motion observation sites in the Kathmandu Valley using strong-motion records from moderate-sized earthquakes," *Earth, Planets and Space*, vol. 69, no. 1, Article ID 23, 2017.

[14] S. D'Amico, A. Akinci, and M. Pischiutta, "High-frequency ground-motion parameters from weak-motion data in the Sicily channel and surrounding regions," *Geophysical Journal International*, vol. 214, no. 1, pp. 148–163, 2018.

[15] V. Hasik, E. Escott, R. Bates, S. Carlisle, B. Faircloth, and M. M. Bilec, "Comparative whole-building life cycle assessment of renovation and new construction," *Building and Environment*, vol. 161, Article ID 106218, 2019.

[16] FEMA, "A practical guide to soil-structure interaction. Soil-structure interaction for building structures NEHRP consultants joint venture a partnership of the applied technology council and the consortium of niversities for research in earthquake engineering," 2003, https://www.ATCouncil.org.

[17] F. M. Wani, J. Vemuri, C. Rajaram, and D. V. Babu, "Effect of soil-structure interaction on the dynamic response of reinforced concrete structures," *Journal of Natural Hazards Research*, vol. 2, no. 4, pp. 304–315, 2022.

[18] J. Wang and J. Yang, "Parametric analysis on the effect of dynamic interaction between nonlinear soil and reinforced concrete frame," *Journal of Applied Sciences*, vol. 12, no. 19, 10.3390/app12199876, Article ID 9876, 2022.

[19] H. A. Awlla, N. R. Taher, and Y. I. Mawlood, "Effect of fixed-base and soil-structure interaction on the dynamic responses of steel structure," *International Journal of Emerging Trends in Engineering Research*, vol. 8, no. 9, pp. 6298–6305, 2020.

[20] S. Tallett-Williams, B. Gosh, S. Wilkinson et al., "Site amplification in the Kathmandu valley during the 2015 M7.6 Gorkha, Nepal earthquake," *Bulletin of Earthquake Engineering*, vol. 14, no. 12, pp. 3301–3315, 2016.

[21] A. Lashgari, M. R. Soghrat, Y. Jafarian, and H. Zafarani, "The 2023 Turkey-Syria earthquake sequence: ground-motion and local site-effect analyses for Kahramanmaras City," *International Journal of Civil Engineering*, vol. 22, no. 5, pp. 877–899, 2024.

[22] A. Aldemir, M. Altuğ Erberik, I. O. Demirel, and H. Sucuoğlu, "Seismic performance assessment of unreinforced sasonry buildings with a hybrid modeling approach," *Earthquake Spectra*, vol. 29, no. 1, pp. 33–57, 2013.

[23] O. Araz, "Optimization of tuned mass damper inerter for a high-rise building considering soil-structure interaction," *Archive of Applied Mechanics*, vol. 92, no. 10, pp. 2951–2971, 2022.

[24] O. Araz, "Optimization of three-element tuned mass damper based on minimization of the acceleration transfer function for seismically excited structures," *Journal of the Brazilian Society*

of Mechanical Sciences and Engineering, vol. 44, no. 10, Article ID 459, 2022.
[25] E. Garini, I. Anastasopoulos, and G. Gazetas, "Soil, basin and soil-building–soil interaction effects on motions of Mexico city during seven earthquakes," *Géotechnique*, vol. 70, no. 7, pp. 581–607, 2020.
[26] C. Amendola and D. Pitilakis, "Large-scale damage assessment of buildings considering SSI and site amplification: the case of Thessaloniki," *Earthquake Spectra*, 2024.
[27] N. Clemett, W. W. C. Gallo, G. J. O'Reilly, G. Gabbianelli, and R. Monteiro, "Optimal seismic retrofitting of existing buildings considering environmental impact," *Engineering Structures*, vol. 250, Article ID 113391, 2022.
[28] T. Cosgun, O. Ceylan, M. M. Nasery et al., "Seismic performance assessment and retrofitting proposal for a historic masonry school building (Bursa, Türkiye)," *Case Studies in Construction Materials*, vol. 18, Article ID e02087, 2023.
[29] C. Michel, A. Karbassi, and P. Lestuzzi, "Evaluation of the seismic retrofitting of an unreinforced masonry building using numerical modeling and ambient vibration measurements," *Engineering Structures*, vol. 158, pp. 124–135, 2018.
[30] A. Scupin and R. Văcăreanu, "Seismic risk reduction through retrofitting of school masonry buildings from Romania," *Frontiers in Built Environment*, vol. 8, 2023.
[31] A. S. Asmone and M. Y. L. Chew, "Development of a design-for-maintainability assessment of building systems in the tropics," *Building and Environment*, vol. 184, Article ID 107245, 2020.
[32] C. Dara, C. Hachem-Vermette, and G. Assefa, "Life cycle assessment and life cycle costing of container-based single-family housing in Canada: a case study," *Building and Environment*, vol. 163, Article ID 106332, 2019.
[33] I. Iervolino, C. Galasso, and E. Cosenza, "REXEL: Computer-Aided Record Selection for Code-based Seismic Structural Analysis," *Bulletin of Earthquake Engineering*, vol. 8, no. 2, pp. 339–362, 2010.
[34] A. R. Kottke, X. Wang, and E. M. Rathje, *Strata Technical Manual*, 2019, https://www.gnu.org/licenses/gpl-3.0-standalone.html.
[35] D. Caicedo, S. Karimzadeh, and V. Bernardo, "Selection and scaling approaches of earthquake time-series for structural engineering applications: a state-of-the-art review," *Archives of Computational Methods in Engineering*, vol. 31, pp. 1475–1505, 2023.
[36] M. N. Fardis, "European structural design codes: seismic actions," in *Encyclopedia of Earthquake Engineering*, M. Beer, I. A. Kougioumtzoglou, E. Patelli, and S. K. Au, Eds., Springer, 2015.
[37] X5 A.X.I.S.V.M.User's Manual, "Technical manual, inter-CAD Mérnöki Szoftverfejlesztő Kft," 2015, https://axisvm.eu/axisvm-products/.
[38] P. Varga, "On the magnitude and possible return period of the historical earthquake in ancient Savaria, 455 AD (Szombathely, West Hungary)," *Austrian Journal of Earth Sciences*, vol. 112, no. 2, pp. 207–220, 2019.
[39] O. Kegyes-Brassai, P. Ray, and R. Kuti, "Seismic risk and disaster management perspectives in Hungary, presented on a case study performed in Győr," *Academic and Applied Research in Military and Public Management Science*, vol. 16, no. 2, pp. 5–16, 2017.
[40] O. Kegyes-Brassai, "*Earthquake hazard analysis and building vulnerability assessment to determine the seismic risk of existing buildings in an urban area (Doctoral dissertation)*," Department of Structural and Geotechnical Engineering, , Széchenyi István University, Győr, 2014.